

Isolation of Rare Cancer Cells from Blood Cells Using Dielectrophoresis

Alireza Salmanzadeh, Michael B. Sano, Hadi Shafiee, Mark A. Stremler, and Rafael V. Davalos*,
IEEE Member

Abstract— In this study, we investigate the application of contactless dielectrophoresis (cDEP) for isolating cancer cells from blood cells. Devices with throughput of 0.2 mL/hr (equivalent to sorting 3×10^6 cells per minute) were used to trap breast cancer cells while allowing blood cells through. We have shown that this technique is able to isolate cancer cells in concentration as low as 1 cancer cell per 10^6 hematologic cells (equivalent to 1000 cancer cells in 1 mL of blood). We achieved 96% trapping of the cancer cells at 600 kHz and 300 V_{RMS}.

I. INTRODUCTION

Circulating tumor cells (CTCs) are rare cells that are shed from tumors during the progression of cancer [1]. There exists strong potential that the investigation of these rare cells will lead to novel cancer treatments and patient-specific medicines. However, isolation and characterization of these cells is arduous due to their low concentration in whole blood [1], which is thought to be fewer than 100 cells per mL [2]. The current state-of-the-art CTC detection methods include fluorescence activated cell sorting (FACS) [3], magnetic bead assisted cell sorting (MACS) [4], and functionalized pillar microchips [2] which use surface or intracellular antibody probes to identify rare cells.

In addition to identification via surface proteins, rare cells can be distinguished and sorted using their intrinsic biophysical and electrical properties [5]. Dielectrophoresis (DEP), the motion of a cell due to non-uniformities in an electric field, is an antibody-free method of cell manipulation [5]. Traditionally, devices employing this phenomenon consist of electrodes patterned on the bottom of a microfluidic channel to generate a non-uniform electric field. Alternatively, insulating structures placed in the path of an otherwise uniform field can be used to constrict current pathways and distort the electric field, a technique referred to as iDEP [6]. These techniques have been successfully used to isolate and enrich DNA, viruses, bacteria, algae, and cells [6].

A technical challenge with these techniques is the direct contact between the electrodes and the sample fluid, which gives rise to the possibility of bubble formation, electrode delamination, and electrode-sample contamination. Contactless dielectrophoresis (cDEP) is an adaption of these techniques that eliminates direct contact between the sample fluid and the metal electrode surface. Instead, two or more

fluid electrode channels, filled with a highly conductive solution, are patterned directly adjacent to a main channel containing the sample. A thin barrier of PDMS, typically 20 μm thick, serves to isolate the fluid electrodes from the sample channel. When an alternating current (AC) voltage is applied across the fluid electrode channels, an electric field is generated within the sample channel.

Recently, cDEP has been used to isolate live cancer cells from beads of similar size [7], dead cells of the live cells of the same cell line [8], live cells from dissimilar cell lines [9], and dilute blood samples [10]. We have demonstrated that this technique can be used to isolate and then culture rare tumor initiating cells from a prostate cancer cell line [11], and that it can potentially be used to identify ovarian cancer from samples of peritoneal fluid [12].

In this study, we demonstrate the ability to trap a low concentration of cancer cells from a sample containing blood cells. MDA-MB-231 breast cancer cells were individually added to a physiologically comparable suspension of hematologic cells in a low conductivity buffer. Observing and counting the cells in inlet and outlet of the device ascertained maximum cancer cell trapping percentage of 96%.

II. THEORY

The time-average DEP force acting on a spherical particle in a non-uniform electric field is given by [5]

$$\vec{F}_{\text{DEP}} = 2\pi\epsilon_m r^3 \text{Re}\{f_{\text{CM}}\} \nabla |\vec{E}_{\text{RMS}} \cdot \vec{E}_{\text{RMS}}|, \quad (1)$$

$$f_{\text{CM}} = \frac{\epsilon_p^* - \epsilon_m^*}{\epsilon_p^* + 2\epsilon_m^*}. \quad (2)$$

where ϵ_m and ϵ_m^* are the real and complex permittivities of the suspending medium, respectively, r is the radius of the particle, ϵ_p^* is the complex permittivity of the particle, and \vec{E}_{RMS} is the root mean square of the electric field. The complex permittivity is defined as $\epsilon^* = \epsilon - \frac{j\sigma}{\omega}$, where ϵ and σ are the real permittivity and conductivity of the particle p or suspending medium m , $j^2 = -1$, and ω is the radial frequency of the electric field. $\text{Re}\{f_{\text{CM}}\}$ is the real part of the Clausius-Mossotti factor, which is a frequency dependent function between -0.5 and 1.

The hydrodynamic drag force on a spherical particle moving in the fluid can be

$$\vec{F}_{\text{Drag}} = 6\eta r \pi (\vec{u}_p / t), \quad (3)$$

*Research supported by National Science Foundation under Grant No. EFRI 0938047 and by the Virginia Tech Institute for Critical Technology and Applied Science (ICTAS).

A. Salmanzadeh, M.B. Sano, H. Shafiee, Ph.D., M.A. Stremler, Ph.D., and R.V. Davalos, Ph.D., are with the Engineering Science and Mechanics Department, Virginia Tech and with the Virginia Tech-Wake Forest University School of Biomedical Engineering and Sciences, Blacksburg, VA 24061 USA (540-231-1979, davalos@vt.edu).

where r is the particle radius, η is the viscosity of the medium, and $\vec{u}_{p/f}$ is the velocity of the particle relative to the medium.

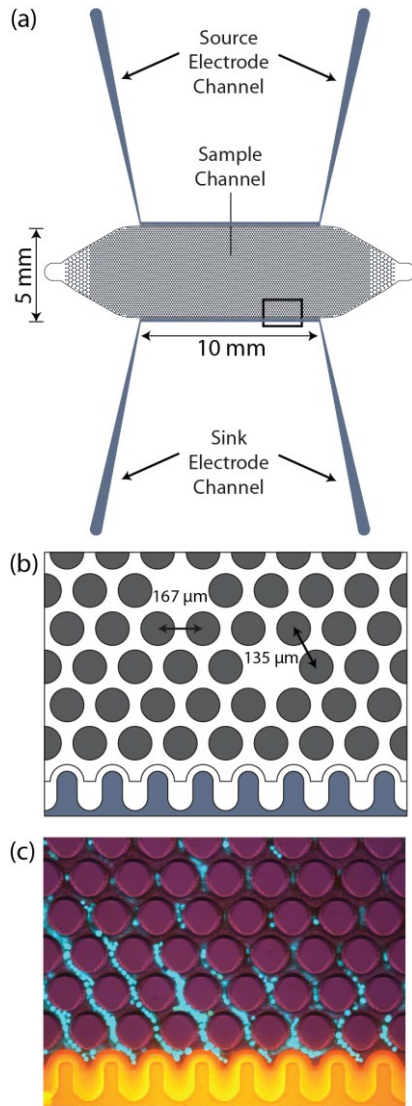


Figure 1. (a - b) Schematic representation of the cDEP microdevice used in this study. The insulating barrier between the sample channel (grey) and the fluid electrode channels (blue) is 20- μ m thick. (c) Breast cancer cells stained with Calcein AM (blue) are trapped due to DEP force. Blood cells which are moving with the background flow, cannot be seen here. More cancer cells were used in to take this figure to make cells more visible. A small amount of Rhodamine B has been added to the PBS in the electrode channels to make them visible.

III. MATERIALS AND METHODS

A. Device layout

Two cDEP devices, shown in Fig. 1(a - b), each with a 5-mm wide, 10-mm long, and 50- μ m deep sample channel, were used in parallel. There are 4000 pillars in each sample channel that produce regions of highly non-uniform electric field in their periphery. Adding the insulating structures allows for wider channels with sufficiently large $\nabla|\vec{E}_{rms} \cdot \vec{E}_{rms}|$, which consequently increases the throughput and selectivity of the devices. Without these pillars, large gradients in the electric field would be limited to areas close

to the side walls of the sample channel, and most cells would not experience a strong enough DEP force to be trapped. The geometry and size of these insulating pillars have been designed to efficient trapping of cancer cells [11].

Using computational modeling (not shown), we found that the channels wider than 5 mm cannot provide high enough $\nabla|\vec{E}_{rms} \cdot \vec{E}_{rms}|$ in the sample channel areas far from electrodes even by using pillars.

Fluid electrode channels are separated from the sample channel by 20- μ m-thick insulating barriers and are filled with phosphate buffered saline (PBS). Electrical connections to the device are made by metal electrodes placed in the inlets of the top and bottom fluid electrodes.

B. Fabrication Process

AZ 9260 photoresist was spun on a silicon wafer. The silicon wafer was exposed to UV light and then the exposed photoresist was removed using AZ 400K developer. Deep Reactive Ion Etching (DRIE) was used to etch the silicon master stamp. To facilitate the stamping process, a thin layer of Teflon was then deposited on the silicon. The liquid-phase PDMS was made by mixing PDMS monomers and a curing agent in a 10:1 ratio. PDMS liquid was poured onto the silicon master, cured for 45 min at 100°C and then removed from the silicon mold. The PDMS replica was bonded with clean glass slides using air plasma. For more details see [11,12].

C. Sample Preparation

Whole blood was collected from a healthy donor and stored in Vacutainer tubes (BD Vacutainer® Sodium Heparin, BD, Franklin Lakes, NJ). The blood was centrifuged for 10 minutes at 3100 RPM (IEC Medilite, Thermo Scientific, Vernon Hills, IL). The high conductivity plasma was aspirated and replaced with the same volume of low conductivity buffer [13]. This process was repeated until the suspension had a conductivity of $120 \pm 5 \mu\text{S/cm}$ as measured with a conductivity meter (Horiba B-173 Twin Conductivity/Salinity Pocket Testers, Cole-Parmer). All experiments were completed within 6 hours after the blood was collected.

Individual samples of human breast cancer cell lines, MDA-MB-231, MCF10A, and MCF7, were used. Details regarding the culturing of these cells are explained in [9]. Cells were stained for visualization with Calcein AM (Invitrogen, Eugene, OR) at a concentration of 2 μL per mL of cell suspension. This staining enabled visualization of the cancer cells in the presence of a large number of red blood cells. The cells were then centrifuged for 5 minutes at 3100 RPM and suspended in low conductivity buffer. The cancer cells and blood sample were then mixed together in one conical tube with a final conductivity of $120 \pm 5 \mu\text{S/cm}$.

D. Experimental Set-Up

Prior to experimentation, devices were stored under vacuum for a minimum of 30 minutes. Upon removal, the sample channel was immediately filled with the sample to maximize the reabsorption of bubbles formed during priming. The two side channels were then filled with PBS and electrodes were placed in the reservoirs connected to the side channels. A 1-mL syringe fastened to a micro-syringe pump

was connected to the inlet of the sample channel with 20 gauge Teflon tubing (Cole-Parmer Instrument Co., Vernon Hills, IL).

A mean fluid velocity of 110 mm s^{-1} was chosen to balance DEP and drag forces so that cells are trapped near the pillars. This velocity corresponds to a flow rate of 0.2 mL/hr in our devices, which was established and maintained for 5 minutes prior to experiments.

The high voltage, high frequency signal was produced using a combination of waveform generation and amplification. The output of a function generator (GFG-3015, GW Instek, Taipei, Taiwan) was fed into a wide band power amplifier (AL-50HFA, Amp-Line Corp., Oakland Gardens, NY) and then passed through a transformer (Amp-Line Corp., Oakland Gardens, NY) to achieve output voltages up to $300 V_{\text{RMS}}$. The output of the transformer was attached to the device through safety microclips (A-MC8-0, Labsmith, Livermore, CA) connected to high voltage rated wires.

After a steady fluid velocity was achieved, a 600 kHz sine wave was applied at voltages between 0 and $300 V_{\text{RMS}}$. An inverted light microscope (Leica DMI 6000B, Leica Microsystems, Bannockburn, IL) equipped with color camera (Leica DFC420, Leica Microsystems, Bannockburn, IL) was used to monitor the cells flowing through the inlet and outlet. The inlet section of the device was observed for 15 minutes and the number of cells observed was counted. Then the outlet section of the device was observed for 15 minutes and the number of cells was again counted. The estimated trapping percentage was then calculated based on the differences in these observations. This process was repeated 3 times for each signal parameter.

Several control experiments were run without applying an electric field, and the number of cells entering the channel were counted and compared to the number of cells leaving the channel per unit of time. In the absence of an applied electric field, fouling of both cancer cells and blood cells was found to be negligible.

IV. COMPUTATIONAL MODELING

The electric field distribution and fluid dynamics were modeled two-dimensionally representation of our domain using COMSOL multi-physics (Version 4.2, COMSOL Inc., Burlington, MA, USA). The electric field distribution and its gradient, $\nabla E = \nabla(\nabla\phi)$, were determined by solving for the potential distribution, ϕ , using the Laplace equation, $\nabla \cdot (\sigma^* \nabla \phi) = 0$, where σ^* is the complex conductivity ($\sigma^* = \sigma + j\omega\epsilon$) of the sub-domains in the microfluidic devices. Uniform potential boundary conditions were applied to the distal edges of the top fluid electrode. A ground boundary condition was applied to the distal edges of the bottom fluid electrode.

The conductivity and permittivity of PDMS was specified in the manufacturer's data sheet as $\sigma_{\text{PDMS}} = 0.83 \times 10^{-12} \text{ S/m}$ and $\epsilon_{\text{PDMS}} = 2.65$. The electrical conductivities of PBS and DEP buffer are $\sigma_{\text{PBS}} = 1.4 \text{ S/m}$ and $\sigma_{\text{DEP}} = 0.01 \text{ S/m}$, respectively, and their relative permittivities are assumed to be $\epsilon_{\text{PBS}} = \epsilon_{\text{DEP}} = 80$ based on their water composition. The electrical properties of PBS and DEP buffer are used for the fluid electrode and sample channels, respectively. The

distributed gradient of the electric field inside the main channel and dielectrophoretic force were investigated for $300 V_{\text{RMS}}$ at 600 kHz .

The COMSOL laminar flow module was used to analyze the fluid velocity field, shear rate and drag force within the sample channel. The inlet velocity was set to 110 mm s^{-1} based on the flow rate in the experiments and the outlet was set to no viscous stress. No-slip boundary conditions were applied to the walls of the channel and the pillars. The viscosity (η) and density (ρ) of the fluid sample were set to $\eta = 0.001 \text{ Pa}\cdot\text{s}$ and $\rho = 1000 \text{ kg/m}^3$, respectively, in the main fluidic channel.

V. RESULTS AND DISCUSSION

A. Computational Results

Computational modeling of the electric field and fluid dynamics were used to estimate device performance (Fig. 2). Our numerical results indicate that $|\vec{E}_{\text{RMS}}|$ is on the order of 10^8 Vm^{-1} and $\nabla|\vec{E}_{\text{RMS}} \cdot \vec{E}_{\text{RMS}}|$ is on the order of $10^{14} \text{ V}^2\text{m}^{-3}$ when $300 V_{\text{RMS}}$ is applied. This level is sufficiently above the required threshold of $10^{12} \text{ V}^2\text{m}^{-3}$ established in previous cDEP studies [14]. Previous investigations on the edge-to-edge separation of pillars found that $\nabla|\vec{E}_{\text{rms}} \cdot \vec{E}_{\text{rms}}|$ has an inverse relation with the distance between the pillars [11]. An edge-to-edge spacing of $25 \mu\text{m}$ was chosen for the experimental device to maximize DEP forces and minimize fouling.

The maximum shear rate in this configuration computed to be 52 s^{-1} [11], well below the established threshold to cause cell lysis of 5000 s^{-1} [15]. The ratio of drag force to DEP force was calculated assuming an average cell radius of approximately $9 \mu\text{m}$ [14] and $f_{\text{CM}} = 1$ [9]. The spatial variation of this ratio is shown in Fig. 2. There are regions on the front and back of each pillar where DEP force is significantly stronger than drag force. We observed that most of the cells were indeed trapped in these DEP-dominant areas (Fig. 1(c)), consistent with the computational results (Fig. 2).

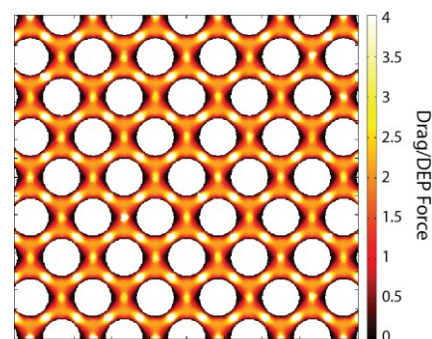


Figure 2. Computational modeling is used to predict the performance of the device. Surface plot of drag force to DEP force ratio.

B. Experimental Results

When a 600 kHz signal was applied, cancer cells began to move toward the pillars. As the voltage was increased cancer cells began to be trapped near the front and back surfaces of the pillars. These regions correspond to the simulated regions of highest $\nabla|\vec{E}_{\text{RMS}} \cdot \vec{E}_{\text{RMS}}|$. In contrast, the red blood cells were mostly unaffected by the DEP force, since that force is

proportional to the cubed radius of the particles. However, a small, un-quantified number of these blood cells were trapped. Samples with cancer cell concentrations of 10^3 cancer cells per mL (10^7 :1 ratio of hematologic to cancer cells) were evaluated. Fig. 3 presents the percentage of MDA-MB-231 cells that were trapped at a constant frequency of 600 kHz and voltages ranging from 0-300 V_{RMS} for concentration of 10^3 cancer cell per 1 mL of suspended blood cells. On average, 96% of MDA-MB-231 cells were trapped at 300 V_{RMS} and 600 kHz at a flow rate of 0.2 mL/hr.

In general, the percentage of cells that are trapped increases by increasing the applied frequency. Thus 600 kHz, the maximum frequency possible with our electronics, was chosen. Future effort should focus on finding the optimal frequency such that target cells receive the optimal DEP response while other cells experience little to no response

Our preliminary results also showed that similar trapping percentages can be achieved for lower concentrations of cancer cells, including 100 cancer cells per mL of blood cells sample as well as other cancer cell lines (data not shown), indicating that this method will potentially work for the detection of many types of cancer cells and in lower concentrations. In our previous studies we showed that the applied electric field does not affect the viability of the cells, and cells can be taken off the chip and cultured after the experiments [11].

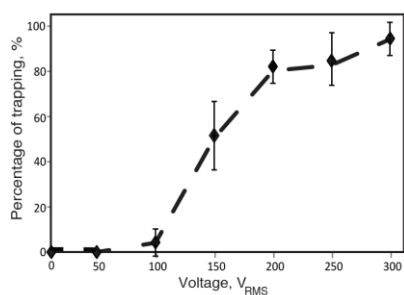


Figure 3. Percentage of trapping of MDA-MB-231 cells at 0-300 V_{RMS} at 600 kHz.

VI. CONCLUSION

In this study, we used a cDEP device that has a high selectivity towards cancer cells, a low selectivity towards red blood cells, high flow rate, and low shear rate. The first two objectives ensure that a majority of cancer cells, which are typically present in low concentrations, can be trapped while preventing clogging due to over-enrichment of red blood cells. A high flow rate is necessary to seek out the hypothesized 10-100 CTCs in each milliliter of patient blood. Finally, a low shear rate is essential for preventing cell damage due to the velocity of the sample fluid. This work shows the potential of cDEP for early diagnosis applications and is the first study using this technique to selectively trap cells present in samples with blood cell concentrations similar to that in whole blood. We will further investigate the selectivity of our technique for isolation of cancer cells versus white and red blood cells in our future studies.

REFERENCES

- [1] M. Yu, *et al.*, "Circulating tumor cells: approaches to isolation and characterization," *The Journal of cell biology*, vol. 192, p. 373, 2011.
- [2] S. Nagrath, *et al.*, "Isolation of rare circulating tumour cells in cancer patients by microchip technology," *Nature*, vol. 450, pp. 1235-U10, Dec 20 2007.
- [3] A. Lostumbo, *et al.*, "Flow cytometry: A new approach for the molecular profiling of breast cancer," *Experimental and Molecular Pathology*, vol. 80, pp. 46-53, Feb 2006.
- [4] K. Kato and A. Radbruch, "Isolation and Characterization of CD34 + Hematopoietic Stem Cells From Human Peripheral Blood by High-Gradient Magnetic Cell Sorting," *Cytometry*, vol. 14, pp. 384-392, 1993.
- [5] H. A. Pohl, *Dielectrophoresis*: Cambridge University Press, 1978.
- [6] S. K. Srivastava, *et al.*, "DC insulator dielectrophoretic applications in microdevice technology: a review," *Anal Bioanal Chem*, vol. 399, pp. 301-21, Jan 2011.
- [7] H. Shafiee, *et al.*, "Selective isolation of live/dead cells using contactless dielectrophoresis (cDEP)," *Lab on a Chip*, vol. 10, pp. 438-445, 2010.
- [8] H. Shafiee, *et al.*, "Selective isolation of live/dead cells using contactless dielectrophoresis (cDEP)," *Lab Chip*, vol. 10, pp. 438-45, Feb 21 2010.
- [9] E. A. Henslee, *et al.*, "Selective concentration of human cancer cells using contactless dielectrophoresis," *Electrophoresis*, vol. 32, pp. 2523-2529, Sep 2011.
- [10] M. B. Sano, *et al.*, "Modeling and development of a low frequency contactless dielectrophoresis (cDEP) platform to sort cancer cells from dilute whole blood samples," *Biosensors & Bioelectronics*, vol. 30, pp. 13-20, Dec 15 2011.
- [11] A. Salmanzadeh, *et al.*, "Isolation of prostate tumor initiating cells (TICs) through their dielectrophoretic signature," *Lab Chip*, vol. 12, pp. 182-189, 2012.
- [12] A. Salmanzadeh, *et al.*, "Dielectrophoretic Differentiation of Mouse Ovarian Surface Epithelial Cells, Macrophages and Fibroblasts using Contactless Dielectrophoresis (cDEP)," *Biomicrofluidics*, 2012.
- [13] L. A. Flanagan, *et al.*, "Unique dielectric properties distinguish stem cells and their differentiated progeny," *Stem Cells*, vol. 26, pp. 656-65, Mar 2008.
- [14] M. B. Sano, *et al.*, "Contactless dielectrophoretic spectroscopy: Examination of the dielectric properties of cells found in blood," *Electrophoresis*, vol. 32, pp. 3164-3171, Nov 2011.
- [15] R. Skalak and S. Chien, *Handbook of bioengineering*. New York: McGraw-Hill, 1987.